Exhibit D

Amplification of MDS1/EVI1 and EVI1, Located in the 3q26.2 Amplicon, Is Associated with Favorable Patient Prognosis in Ovarian Cancer

Meera Nanjundan,[1] Yasuhisa Nakayama,[1] Kwai Wa Cheng,[1] John Lahad,[1] Jinsong Liu,[2] Karen Lu,[3] Wen-Lin Kuo,[4] Karen Smith-McCune,[5] David Fishman,[6] Joe W. Gray,[4] and Gordon B. Mills[1]

Departments of [1]Molecular Therapeutics, [2]Pathology, and [3]Gynecologic Oncology, M. D. Anderson Cancer Center, University of Texas, Houston, Texas; [4]Department of Laboratory Medicine, University of California, San Francisco, and the Lawrence Berkeley National Laboratory, Berkeley, California; [5]Department of Obstetrics, Gynecology, and Reproductive Sciences, University of California, San Francisco, California; and [6]New York University, New York, New York

Abstract

Increased copy number involving chromosome 3q26 is a frequent and early event in cancers of the ovary, lung, head and neck, cervix, and BRCA1 positive and basal breast cancers. The p110α catalytic subunit of phosphoinositide-3-kinase (PI3KCA) and protein kinase Cι (PKCι) have previously been shown as functionally deregulated by 3q copy number increase. High-resolution array comparative genomic hybridization of 235 high-grade serous epithelial ovarian cancers using contiguous bacterial artificial chromosomes across 3q26 delineated an ~2 Mb–wide region at 3q26.2 encompassing PDCD10 to MYNN (chr3:168722613-170908630). Ecotropic viral integration site-1 (EVI1) and myelodysplastic syndrome 1 (MDS1) are located at the center of this region, and their DNA copy number increases are associated with at least 5-fold increased RNA transcript levels in 83% and 98% of advanced ovarian cancers, respectively. Moreover, MDS1/EVI1 and EVI1 protein levels are increased in ovarian cancers and cancer cell lines. EVI1 and MDS1/EVI1 gene products increased cell proliferation, migration, and decreased transforming growth factor-β–mediated plasminogen activator inhibitor-1 promoter activity in ovarian epithelial cells. Intriguingly, the increases in EVI1 DNA copy number and MDS1/EVI1 transcripts are associated with improved patient outcomes, whereas EVI1 transcript levels are associated with a poor patient survival. Thus, the favorable patient prognosis associated with increased DNA copy number seems to be as a result of high-level expression of the fusion transcript MDS1/EVI1. Collectively, these studies suggest that MDS1/EVI1 and EVI1, previously implicated in acute myelogenous leukemia, contribute to the pathophysiology of epithelial ovarian cancer. [Cancer Res 2007;67(7):3074–84]

Introduction

In the United States in 2006, the American Cancer Society predicts that 20,180 women will develop ovarian cancer, and 15,310 will die of their disease. Ovarian cancer has proven to be a powerful model for the identification and characterization of aberrant genes contributing to the pathophysiology of ovarian cancer as well as multiple other cancer lineages. Thus, identification and characterization of genomic aberrations and of their drivers will increase our understanding of the initiation and progression of cancer as well as provide molecular markers that could improve early cancer detection, determining prognosis, and predicting response to therapy. Increased copy number involving chromosome 3q26 is a frequent and early event in a number of epithelial cancers, including squamous cell carcinomas (SCC) of the cervix (1), esophagus (2, 3), lung (1), head and neck (4), prostate cancer (5, 6), breast cancer (basal and BRCA1-associated; refs. 7, 8), and nasopharyngeal cancer (9), as well as in chronic myelogenous leukemia (10). The 3q amplification domain has been variously identified as 3q26 ~ 27, q25 ~ 26, and q26 ~ qter by various low-resolution methods with the minimum region of overlap identified spanning nearly 20 Mb, making it challenging to search for possible target genes.

A number of potential targets in the 3q26 amplicon have been identified in epithelial cancers through these low-resolution approaches, including PIK3CA [catalytic subunit of phosphoinositide-3-kinase (PI3K); ref. 11], protein kinase Cι (PKCι; refs. 12–14), eukaryotic initiation factor (15), ZASC1 (a novel Kruppel-like zinc finger protein; ref. 2), SnoN (3), SCC-related oncogene (16), and TERC (RNA component of human telomerase; ref. 17). These studies suggest that 3q26 may contain one or more putative oncogenes, which play important roles in the development or the progression of various solid tumors.

In ovarian cancers, the p110α catalytic subunit of PIK3CA (11) and PKCι (12) are functionally deregulated by 3q copy number increase. However, the 3q26 region contains other candidates, including ecotropic viral integration site-1 (EVI1). A recent report indicates that EVI1 is amplified at 3q26, resulting in increased RNA levels that may contribute to aberrant transforming growth factor-β (TGFβ) signaling in ovarian cancer (18). EVI1 has been implicated in acute myelogenous leukemia (AML) and myelodysplastic syndrome (MDS), where it is frequently activated due to intra- and interchromosome rearrangements. EVI1 has been implicated in proliferation of leukemic cells, transformation of Rat1 fibroblasts, inhibition of growth factor-mediated differentiation and survival, induction of neural and megakaryocyte differentiation, and inhibition of TGFβ signaling (19). EVI1 also

Note: Supplementary data for this article are available at Cancer Research Online (http://cancerres.aacrjournals.org/).

M. Nanjundan and Y. Nakayama contributed equally to this manuscript.

The M. D. Anderson Cancer Center, Department of Molecular Therapeutics, University of Texas and the Department of Laboratory Medicine, University of California San Francisco and the Lawrence Berkeley National Laboratory, Berkeley, California are equal contributors.

Current address for Y. Nakayama: Department of Pharmacology, Kansai Medical University, 10-15 Fumizono-cho, Moriguchi City, Osaka 570-8506, Japan.

Requests for reprints: Meera Nanjundan, M. D. Anderson Cancer Center, Department of Molecular Therapeutics, University of Texas, 1515 Holcombe Boulevard, Box 0950, Houston, TX 77054. Phone: 713-563-4225; Fax: 713-563-4235; E-mail: mnanjund@mdanderson.org.

doi:10.1158/0008-5472.CAN-06-2366

(*a*) blocks mothers against DPP homolog (SMAD)–induced gene transcription through binding to SMAD3, (*b*) enhances activator protein 1 activity, (*c*) blocks c-jun-NH_2-kinase and stress-induced apoptosis, (*d*) blocks the action of IFN by blocking promyelocytic leukemia (PML) function, and (*e*) binds the brahma-related tumor suppressor, BRG1 (19), and more recently, is implicated in signaling through the PI3K/AKT pathway (20). We now use a high-resolution array comparative genomic hybridization (CGH) bacterial artificial chromosome (BAC) contig to show that EVI1 is located at the most frequent point of genomic amplification at 3q26.2 in 235 advanced serous epithelial ovarian cancers. Specifically, we show that DNA copy number increase is associated with marked accumulation of MDS1/EVI1 (PRDM3) intergenic read-through transcripts and MDS1 and EVI1 transcripts. MDS1/EVI1 and EVI1 functionally dysregulate cellular proliferation, gene transcription, and cellular motility. Intriguingly, the increases in DNA copy number and MDS1/EVI1 transcripts are associated with improved patient outcomes, whereas EVI1 is associated with a worsened outcome. These studies show that MDS1/EVI1 and EVI1, previously implicated in AML, contribute to the pathophysiology of epithelial ovarian cancers.

Materials and Methods

Preparation of patient samples. Stages I to IV serous epithelial ovarian cancers were from the Ovarian Cancer Tumor Bank of the M.D. Anderson Cancer Center. Benign ovarian cysts and stages III and IV serous epithelial ovarian cancers were from the Basic Biology of Ovarian Cancer Program Project Grant Bank at the University of California, San Francisco. Benign ovarian cysts were macrodissected to increase the amount of epithelium present. Early-stage and late-stage ovarian cancers were macrodissected to contain >70% tumor. Normal ovarian epithelial scrapings were from the Northwestern University. Normal scrapings were collected using a cytobrush, and cells immediately suspended and frozen in RLT buffer (Qiagen, Valencia, CA). DNA was extracted as previously described (21). Total RNA was extracted from ovarian cancers and normal ovarian epithelial scrapings using the RNeasy Kit (Qiagen, Valencia, CA) according to the manufacturer's protocol. Institutional Review Board approval was obtained at each institution before the initiation of this study.

Comparative genomic hybridization and analysis. CGH was done with a 3q BAC contig as previously described (21). Only BACs with signals in 90% or greater of tumors are included. In the CGH data set presented in Fig. 1*A*, there were five BACs containing EVI1. The EVI1 signal is represented as the average copy number change across the five BACs. The values are depicted using a $\log_2$-based color scale (as indicated), such that the red reflects increased copy number and blue reflects decreased copy number. Light green indicates a null data point either as a result of poor hybridization and quality control or as a result of a probe not being analyzed for that sample.

***In vitro* methylation assay.** MDS1/EVI1-HA, EVI1-HA, and AKT-HA (used as negative control) were transiently expressed in COS7 cells and immunoprecipitated using HA antibody. Sepharose G-beads containing immunoprecipitates and GST-PRMT1 (used as positive control; kind gift of Dr. Mark Bedford, M.D. Anderson Cancer Center) were incubated with 2 μCi of 1 mCi/mL ^{3}H-*S*-adenosyl-L-methyl-^{3}H-methionine, 10 μg histones in Tris-HCl buffer for 2 h at 37°C. The reactions were terminated by adding SDS sample buffer and boiled. Samples were run on a 15% SDS-PAGE gel, which was stained with Gelcode Blue (Pierce, Rockford, IL), destained, soaked in Enhance (Perkin-Elmer, Waltham, MA), washed, vacuum dried, and then exposed to film overnight at −80°C.

Quantitative PCR analysis. Quantitative PCR was done using RNA isolated from normal, benign, early-stage (I and II), and advanced-stage (III and IV) patient ovarian samples using a one-step reverse transcription-PCR TaqMan master mix kit (Applied Biosystems, Foster City, CA) with the following primers and probes sets:

EVI1 exon III (detects both EVI1 and MDS1/EVI1): forward primer, CGAAGACTATCCCCATGAAACTATG; reverse primer, TCACAGTCTTCGCAGCGATATT; probe sequence: TCCACGAAGACGGA.

EVI1 exon I: (detects only EVI1) forward primer, TTGCCAAGTAACAGCTTTGCTG; reverse primer, CCAAAGGGTCCGAATGTGACTT; probe sequence: TCGCGAAGCAGCACAC.

MDS1/EVI1: forward primer, TCAAACCTGAAAGACCCCAGTTA; reverse primer, GCATCTATGCAGAACTTCACATTGT; probe sequence: TGGATGGGAGATCTT.

MDS1: forward primer, AACCTGAAAGACCCCAGTTATGG; reverse primer, CGCTTACCCTCCGAGACCTT; probe sequence: ATGGGAGGTACATCTT.

The MDS1 qPCR probe recognizes a domain that is not included in the MDS1/EVI1 fusion gene (see Fig. 1*B* for details). However, the EVI1 exon III qPCR probe recognizes both EVI1 and MDS1/EVI1 (designated as "EVI1 + MDS1/EVI1"). The MDS1/EVI1 qPCR probe recognizes the mRNA fusion site and is specific to MDS1/EVI1. The EVI1 exon I qPCR probe is designed to specifically recognize EVI1 and not the fusion transcript, MDS1/EVI1 (designated as "EVI1"). Primers/probes for all of the remaining genes in the EVI1 region were based on corresponding Genebank sequences (Applied Biosystems, Assays by Design). Using the correlative method, RNA-fold increase in expression was calculated as Ct of gene − Ct of β-actin to generate ΔCt from which ΔCt of the normal sample was subtracted. These values were then converted to $\log_2$ values.

Plasmid constructs. EVI1 and MDS1/EVI1-HA fusion constructs were provided kindly by Rotraud Wieser (KIMCL, Abteilung fuer Humangenetik, Medizinische Universitaet Wien, Wien, Austria; ref. 22). EVI1 was kindly provided by Dr. Hisamaru Hirai (23) and Dr. Mineo Kurokawa (Department of Hematology and Oncology, Graduate School of Medicine, University of Tokyo, Tokyo, Japan; ref. 23).

SDS-PAGE and Western blot analysis. Proteins were resolved on an 8% SDS-PAGE gel and electrophoretically transferred to polyvinylidene difluoride membranes. After blocking with 5% (w/v) milk, membranes were incubated overnight at 4°C with primary antibody and 1 h with appropriate horseradish peroxidase-conjugated secondary antibodies. Blots were developed using chemiluminescence substrates (GE Healthcare, Piscataway, NJ). Polyclonal EVI1 antibody was obtained from Dr. Hisamaru Hirai recognizing amino acid 1 to 263 (24) and from Dr. James Ihle (Department of Biochemistry, St. Jude Children's Research Hospital, Memphis, TN; ref. 25).

Proliferation and cellular migration assays. IOSE80 and IOSE29 htert immortalized ovarian cells (T80/T29) were transfected with EVI1 and MDS1/EVI1 by Nucleofector method using T solution (Amaxa, Gaithersburg, MD). The transfection efficiency was ~60% to 80% assessed by enhanced green fluorescent protein (EGFP) fluorescence. After 12 h, cells were counted, and 5,000 cells were plated in 96-well plates maintained in 0% or 10% fetal bovine serum (FBS). At various days, cells were fixed and stained with crystal violet solution, dissolved in Sorenson's buffer, and absorbance was measured at 570 nm. Twenty-four hours after transient transfection, cells were harvested, counted, and seeded into Boyden chamber inserts (BD Biosciences, San Jose, CA) in serum-free media. FBS in the lower chamber media was used as a chemoattractant. The cells that migrated onto the lower membrane were stained with crystal violet and counted.

Statistical analysis. Experimental results were statistically evaluated using Student's *t* test. Differences were considered significant if $P < 0.05$. Patients with no further follow-up information are represented by a vertical tick at last point contact and are weighed in the Kaplan-Meier analysis.

Results

Delineation of the 3q26.2 amplicon in ovarian cancer. Increased copy number involving chromosome 3q26.2 is a frequent and early event in ovarian cancer development and is found in a subset of other epithelial cancers. The driver(s) of the regional DNA copy number increase on chromosome 3q and in particular at 3q26

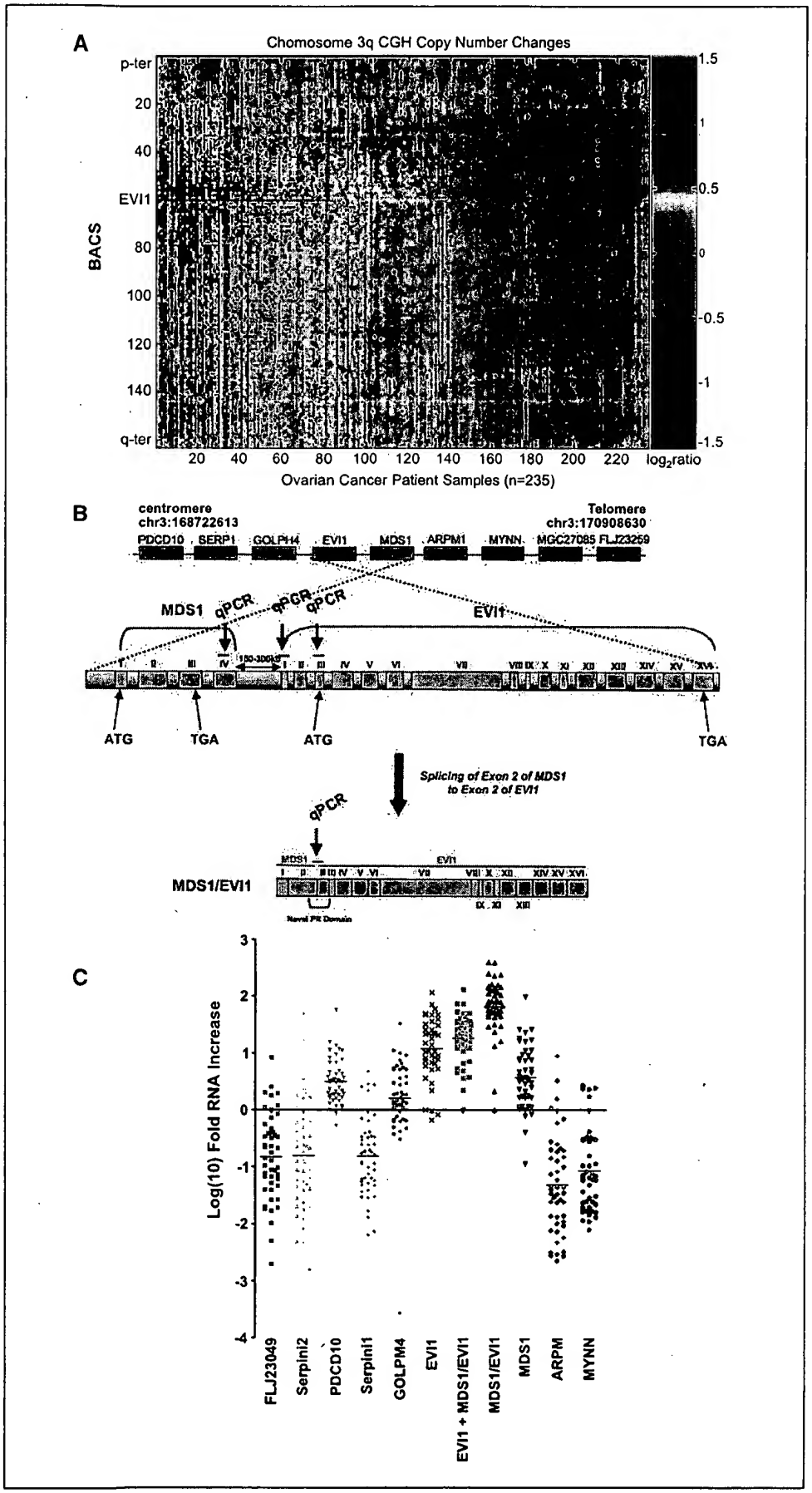

Figure 1. EVI1 genomic copy number increase is associated with a selective accumulation of EVI1 and MDS1/EVI1 transcripts. *A*, CGH analysis for 235 ovarian tumors using a contig encompassing 163 BACs probes on 3q is shown as a scaled image map. The signal for the EVI1 BAC is the maximum signal intensity across the group of BACs for EVI1 region. The patient samples are ordered with respect to decreasing EVI1 copy number alterations from left to right. The BACs on chromosome 3q are ordered by position along the chromosome. Parametric and nonparametric correlation analyses were done to delineate the region of highest correlation on 3q. Data vectors for each BAC on chromosome 3q were created, and correlation coefficients were determined for each BAC compared with every other BAC on the chromosome. The region on 3q from PDCD10 to MYNN (Chr3:168722613-170908630) was the most frequently altered area on 3q when compared with the frequency of change for other regions. In addition, BACs within this region exhibited the most statistically significant direct correlation with other BACs in the region. *B*, genomic organization surrounding MDS1 and EVI1. Open reading frames within the minimally aberrant region on 3q are organized from centromere to telomere. MDS1 and EVI1 as well as the MDS1/EVI1 intergenic read-through are shown in detail. The MDS1/EVI1 intergenic transcript contains exon I and exon II of the MDS1 coding sequence, followed by the untranslated region of EVI1 (exon II), respectively, giving rise to a novel PR domain and the complete open reading frame of EVI1. The location of the qPCR primers for MDS1 (exon IV), MDS1/EVI1 (PR domain), and EVI1 (two independent probe sets: one against exon I and the other against exon III) are indicated. *C*, RNA expression levels of genes surrounding EVI1 along chromosome 3q, from PDCD10 to MYNN, were assessed by quantitative PCR (qPCR) analysis in ovarian tissue samples. The results are displayed as $\log_{10}$-fold RNA alterations for NOE and advanced tumors (stages III and IV), compared with the average of the normal epithelium. The EVI1 exon I probe is specific for EVI1 alone (specifically EVI1d), the EVI1 exon III probe recognizes both EVI1 and MDS1/EVI1 levels (denoted as EVI1 + MDS1/EVI1), whereas the MDS1/EVI1 probe is specific to the fusion gene. *PDCD10*, programmed cell death 10; *Serpini1*, a serine/cysteine proteinase inhibitor, *GOLPH4*, Golgi phosphoprotein 4, *ARPM1*, an actin-related protein, and *MYNN*, myoneurin zinc finger protein.

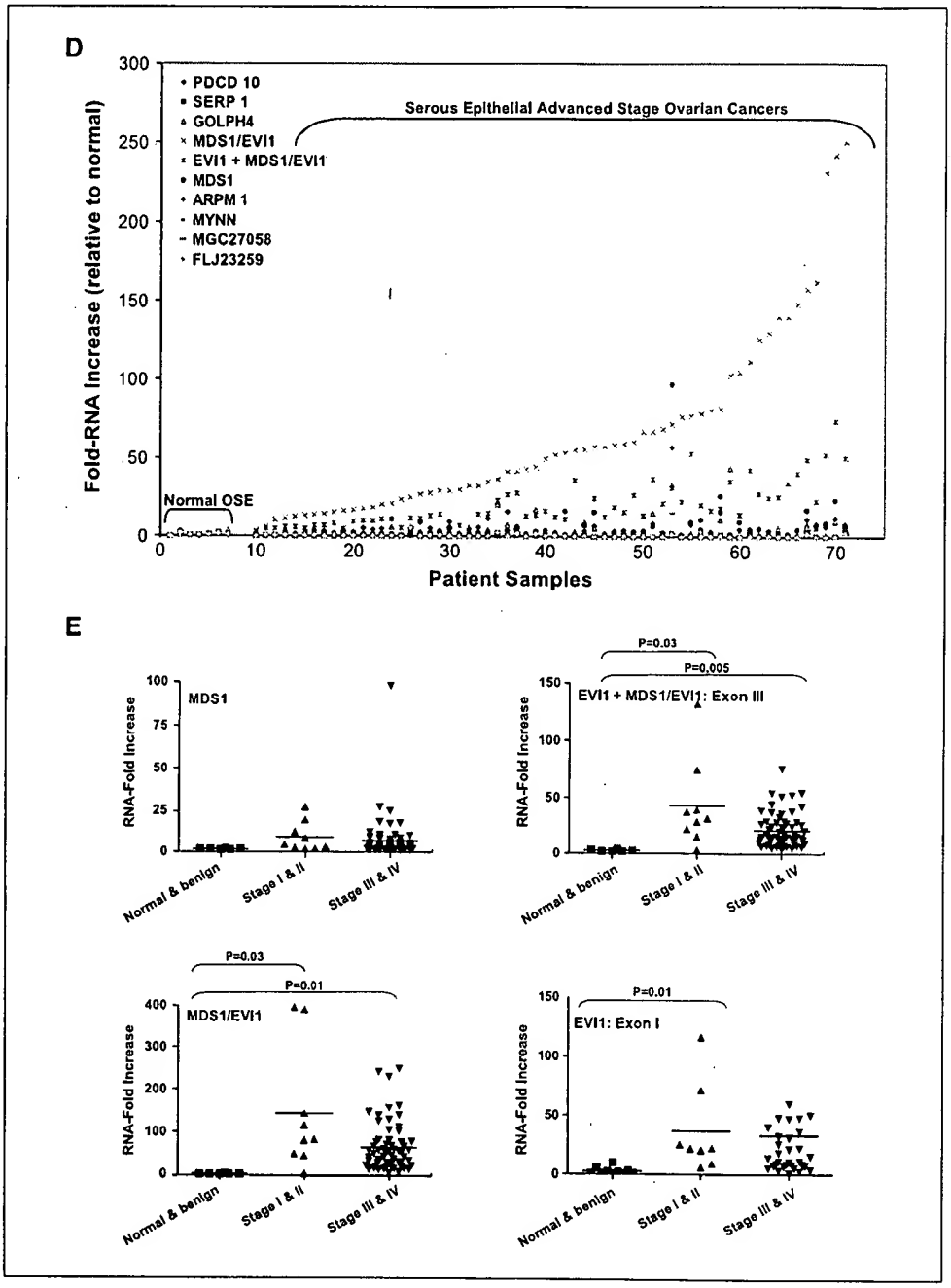

Figure 1 *Continued.* *D*, the results from (*C*) are displayed as fold RNA for normal OSE and serous epithelial advanced stage ovarian cancers. EVI1 in this graph is shown using exon III probe (*EVI1 + MDS1/EVI1*). *E*, RNA expression levels of total EVI1 and MDS1/EVI1 (exon III qPCR probes), EVI1 (exon I qPCR probes), MDS1/EVI1, and MDS1 were assessed by quantitative PCR analysis in ovarian tissue samples by stage as fold alterations in RNA expression compared with that of normal epithelium. Normal and benign cystadenomas, stages I and II, as well as stages III and IV, were grouped together to increase sample size. Both stage I/II and stage III/IV were significantly increased from normal/benign.

in epithelial cancers remain to be fully characterized. PI3K (11) and PKCι (12, 13) both have been reported to be elevated at the mRNA and protein levels in association with the 3q copy number increase in ovarian cancer. However, the region of copy number increase defined in earlier low-resolution CGH studies extended over much of 3q, suggesting that additional genes likely contribute to the selection of the amplicon.

Thus, to better define aberration structure within the 3q26 region, we applied high-resolution array CGH to 235 high-grade serous epithelial ovarian cancers using a contig encompassing 163 contiguous BACs across 3q (Fig. 1*A*). The levels of amplification and deletion varied dramatically between different patients, but several occurred frequently, suggesting that they contribute to the pathophysiology of ovarian cancer. The complex pattern of changes suggests that multiple different drivers exist for the 3q26 amplicon. We more clearly defined and narrowed the most frequent region of copy number increase in ovarian cancers to an ~2 Mb-wide region at 3q26.2 encompassing FLJ23049 to MYNN (chr3:168722613-170908630; Fig. 1*A*) that is aberrant in >70% of all serous epithelial ovarian cancers. As noted in Fig. 1*A*, aberrations involving other regions of 3q26 also were observed, including those present in tumors lacking the increase at 3q26.2 but at lower frequency than the aberration encompassing FLJ23049 to MYNN. MDS1 and EVI1 are located at the center of the chr3:168722613-170908630 region representing the most aberrant loci in the region. Three additional ovarian CGH data sets of 50, 72, and 86 patient samples confirmed that this region and specifically MDS1 and EVI1 showed selective amplification in ~70% of patients (data not

presented). In support, previous reports have indicated increased EVI1 DNA or RNA levels in ovarian cancer (18, 26).

To identify mutations within EVI1, we sequenced EVI1 from genomic DNA across its 16 exons in 48 ovarian cancer patients. Out of 48 patients, 2 patients had a nonsynonymous mutation in exon 14 of EVI1. In addition, a common synonymous mutation in exon 13 was observed in ~25% of the patients, which is a previously documented single nucleotide polymorphism. Thus, the frequency of mutations/sequence changes is <4%, with no obvious functional effect expected arising from the mutations in exon 14.

Increased EVI1 copy number is associated with elevated EVI1 and MDS1/EVI1 transcripts in ovarian cancers. To assess whether the observed DNA copy number increase in EVI1 corresponds to increased transcript levels, quantitative PCR (qPCR) analysis of nine genes encoded in chr3:168722613-170908630 in the 3q26.2 amplicon was done (see Fig. 1*B* for genomic organization of this region). In addition, we assessed the transcript expression level of the MDS1/EVI1 intergenic fusion transcript (see Fig. 1*B* for details). We designed several qPCR probes to assess the level of EVI1, MDS1, and the fusion transcript MDS1/EVI1. As shown in Fig. 1*B*, the EVI1 exon I probe specifically recognizes only EVI1, the MDS1 qPCR probe (against exon IV of MDS1) is specific for MDS1, EVI1 exon III recognizes EVI1 as well as MDS1/EVI1 (designated as EVI1 + MDS1/EVI1), whereas the MDS1/EVI1 probe is specific to the intergenic novel domain in the fusion transcript, MDS1/EVI1.

To determine whether the 3q26.2-amplified gene transcript levels were elevated in advanced-stage ovarian cancers relative to ovarian surface epithelium, we assessed their expression in 61 advanced-stage serous epithelial ovarian cancers (>70% tumor) and 7 normal ovarian epithelium (NOE) obtained by scraping epithelial cells directly into RNA later. Thus, comparing NOE to ovarian cancers, we observed a centromeric regional increase resulting in selective accumulation of EVI1, EVI1 + MDS1/EVI1, and MDS1/EVI1 intergenic fusion transcripts (Fig. 1*C*, presented as $\log_{10}$-fold RNA increases). Specifically, transcript levels of other genes assessed did not differ significantly between NOE and advanced-stage ovarian cancers other than a modest increase in MDS1, PDCD10, and GOLPH4. Thus, EVI1 and MDS1/EVI1 represent the most highly and frequently amplified transcripts within this region. MDS1/EVI1 and EVI1 exon III (EVI1 + MDS1/EVI1) RNA levels are increased up to 540- and 125-fold in the majority (98% and 83%) of ovarian cancers, respectively (Fig. 1*D*, presented as RNA-fold increases) relative to NOE. In addition, transcriptional profiling using probes that do not distinguish between EVI1 and MDS1/EVI1 in two independent data sets of 69 and 30 samples also indicated that total EVI1 and MDS1/EVI1 were the most frequently and markedly amplified transcripts in the 3q26.2 region (not presented). Furthermore, previous studies have indicated elevated RNA levels for EVI1 using approaches that would not distinguish between EVI1 and MDS1/EVI1 in ovarian cancer (18, 26).

To determine whether EVI1 mRNA was selectively elevated in ovarian cancer, we used probes to exon I (see Materials and Methods), which distinguishes between EVI1 and the fusion transcript MDS1/EVI1 (27) to assess EVI1d transcript levels (Fig. 1*C*). We found that the relative fold increases of the EVI1 exon I probe were similar to the EVI1 exon III probe. Thus, both EVI1 and MDS1/EVI1 transcripts are highly elevated in ovarian cancers.

RNA expression levels of EVI1 and MDS1/EVI1 were further assessed by qPCR analysis in ovarian tissue samples by stage. RNA levels for MDS1, EVI1, and MDS1/EVI1 were elevated compared with normal and benign cystadenomas in both early (stages I and II) and late stages of ovarian cancer (stages III and IV; Fig. 1*E*). Benign cystadenomas were macrodissected to enrich for epithelial cells; however, contamination with stromal cells is still present accounting for the majority of cells. Nonetheless, the comparison to cysts supplements the data from purified ovarian epithelial cells, indicating that EVI1 and MDS1/EVI1 levels are increased in ovarian cancers.

The increases in RNA levels for EVI1 and MDS1/EVI1 were much greater than the increases in DNA copy number in both magnitude and frequency (compare $\log_2$ scale in Fig. 1*A* to $\log_{10}$ scale in Fig. 1*C*). Thus, there exist additional alterations other than increased DNA copy number that may lead to the observed increased RNA expression levels, including rearrangements/mutations involving regulatory regions or epigenetic alterations. Nonetheless, the overall patterns of gene amplification and elevated gene expression are concordant where highly amplified genes are highly expressed. EVI1 and the MDS1/EVI1 "read-through" transcript seem to be major drivers of the 3q26.2 aberration and, thus, may play important roles in the initiation and/or progression of ovarian cancers. The MDS1/EVI1 fusion mRNA is selectively elevated in serous epithelial ovarian cancers, indicating that the MDS1/EVI1 fusion may play a novel role in ovarian cancer pathogenesis.

Increased EVI1 transcripts are associated with elevated EVI1 and MDS1/EVI1 protein in ovarian cancer cell lines and advanced cancers. To assess whether increased EVI1 and MDS1/EVI1 transcript levels result in an increase in protein, Western blot analysis was done across a series of ovarian cell lines and advanced-stage ovarian cancers. CGH profiles of SKOV3 and OVCAR8 cells are shown in Fig. 2*A*, where EVI1 is amplified at the 3q26.2 locus in SKOV3 cells and homozygously deleted in OVCAR8 cells, providing positive and negative controls. Western blot analysis was done in SV40/htert immortalized ovarian surface epithelial cells (T80), SKOV3, and OVCAR8 cell lines using a polyclonal antibody (from Dr. Hirai; ref. 23), recognizing both EVI1 and MDS1/EVI1 forms. EVI1 and MDS1/EVI1 protein were present at low levels in T80, markedly elevated in SKOV3, and absent in OVCAR8, which closely parallel transcript levels in cell lines (Fig. 2*B*).

Using an EVI1 polyclonal antibody (from Dr. J. Ihle; ref. 25), recognizing both EVI1 and MDS1/EVI1, we assessed protein expression level of EVI1 and MDS1/EVI1 in SKOV3, OVCA429, HEY, DOV13, OVCAR8, and T80 cells. Western blot analysis shows high-level EVI1 expression in SKOV3 cells, its absence in OVCAR8, and low expression in T80 cells. MDS1/EVI1 and EVI1 protein levels were found to closely parallel transcript levels and DNA copy number in a number of ovarian cancer cell lines as shown in the corresponding qPCR analysis with DNA copy number (by fluorescence *in situ* hybridization analysis; Fig. 2*C*).

In advanced ovarian patient samples, using the antibody from Hirai (23), densitometric analysis of EVI1 and MDS1/EVI1 levels in advanced-stage ovarian cancer patients showed that MDS1/EVI1 and EVI1 protein were increased relative to T80 (Fig. 2*D*). MDS1/EVI1 protein levels seem increased relative to wild-type EVI1 in these ovarian cancers, with most cancers expressing low to undetectable levels of wild-type EVI1. In these patient samples, EVI1 transcripts and protein correlated with MDS1/EVI1 transcripts ($P = 0.0001$) and protein ($P = 0.0031$) in contrast to MDS1 where there was no correlation (not presented). However, transcript levels did not correlate with protein levels for either EVI1 and MDS1/EVI1, suggesting that additional mechanisms exist accounting for the high levels of these proteins, including rearrangements, effects of enhancers and promoters, fusion products, mRNA, and

protein stability. Thus, the protein expression profiles support EVI1 and/or MDS1/EVI1 as contributing to the effect of the recurrent regional DNA copy number increase on chromosome 3q26.2 in the pathophysiology of ovarian cancer.

Short-term EVI1 overexpression promotes ovarian cell proliferation, migration, and represses TGFβ-mediated PAI-1 transcriptional regulation in ovarian cells. Because MDS1/EVI1 and EVI1 transcripts seemed to be the most abundant transcripts in advanced-stage ovarian cancers in the 3q26.2 amplicon, we next investigated whether certain components of the epithelial-mesenchymal transformation (EMT) process (cell proliferation and migration) required during epithelial tumor initiation and progression may be altered as a result of aberrant expression of EVI1 and MDS1/EVI1 in T80 cells. We first assessed the role of EVI1 and MDS1/EVI1 on ovarian cell proliferation by transient transfection by Nucleofector method into T80 cells. Transfection of HA-tagged EVI1 and MDS1/EVI1 into T80 cells was assessed by Western blot analysis (Fig. 3*A*) as well as nuclear fluorescence (transfection efficiency of ~60–80% based on nuclear EGFP fluorescence; Fig. 3*B*). We observed that wild-type EVI1 and MDS1/EVI1 increased cell proliferation and saturation density of cells grown in the presence (10%) or absence (0%) of FBS (Fig. 3*C*). Moreover, transient expression of EVI1 in the ovarian cancer cell line, OVCAR8 (with >50% transfection efficiency), which contains a deletion at the EVI1 locus, failed to alter growth or cell cycle relative to control transfected cells.

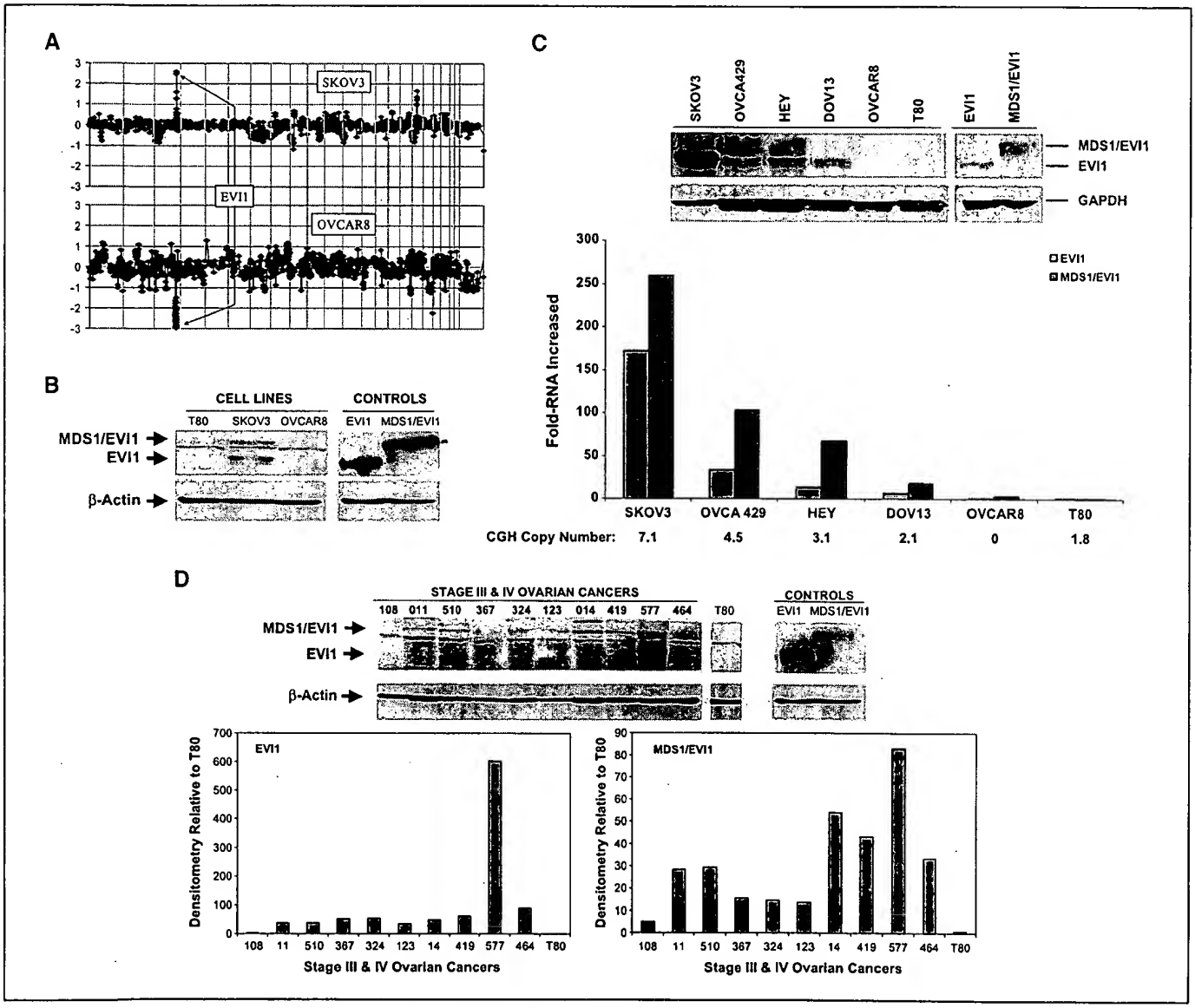

Figure 2. EVI1 genomic copy number increase is associated with a selective accumulation of EVI1 and MDS1/EVI1 protein. *A*, CGH profiles of SKOV3 and OVCAR8 cells are displayed showing EVI1 amplified at the 3q26.2 locus in SKOV3 cells and deleted in OVCAR8 cells. *B*, Western analysis was done in T80, SKOV3, and OVCAR8 cell lines and with EVI1 and MDS1/EVI1 transfected in T80 cells as positive controls (*CONTROLS*) using polyclonal antibody recognizing both EVI1 and MDS1/EVI1. β-Actin was used as loading control. *C*, Western analysis was done in SKOV3, OVCA429, HEY, DOV13, OVCAR8, and T80 cells and with EVI1 and MDS1/EVI1 transfected in T80 cells as positive controls (*CONTROLS*) using an antibody that recognizes both EVI1 and MDS1/EVI1. qPCR for EVI1 and MDS1/EVI1 was done in ovarian cell lines. The results are displayed as fold-RNA expression normalized to T80; CGH copy number for the cell lines is indicated below the lines. Experiments were done in triplicate. *D*, Western analysis of EVI1 was done using the antibody that recognizes both EVI1 and MDS1/EVI1 in advanced ovarian patient samples. T80 cells transfected with EVI1 and MDS1/EVI1 were used as positive controls. Densitometric analysis of EVI1 and MDS1/EVI1 levels in advanced-stage ovarian cancer patients normalized to T80 protein is presented.

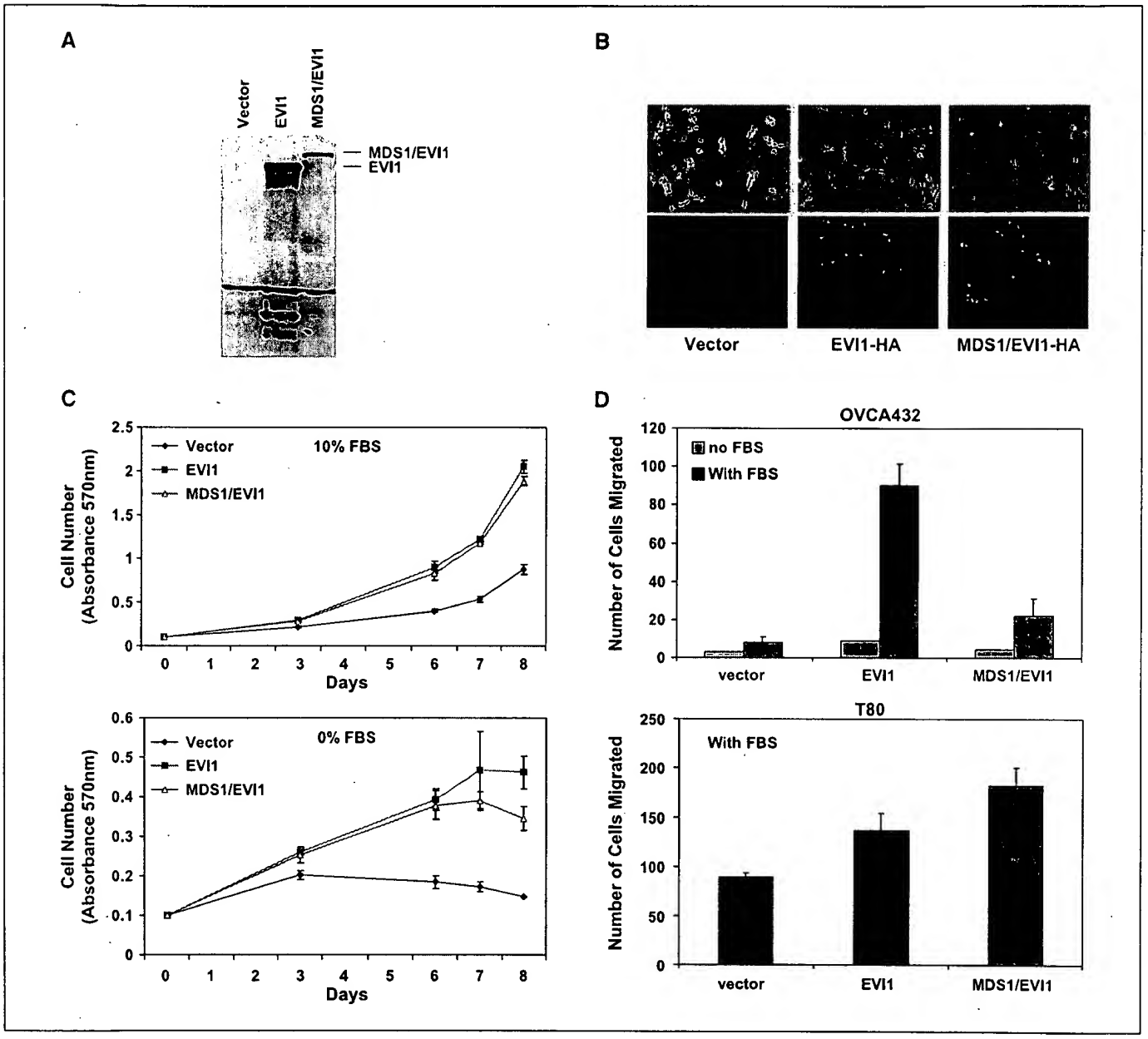

Figure 3. EVI1 and MDS1/EVI1 alter ovarian cell–proliferative and migratory responses. *A*, EVI1 and MDS1/EVI1 were overexpressed in T80 cells. Lysates were harvested, and Western analysis was done using Hirai's polyclonal antibody. *B*, EVI1-HA and MDS1/EVI1-HA were overexpressed in T80 cells and stained for HA to visualize nuclear overexpression. *C*, effect of EVI1 and MDS1/EVI1 on proliferation of T80 cells was done in 10% FBS (*top*) and 0% FBS (*bottom*). The growth assay was done in 96-well plates where cells were plated at 5,000 cells per well and grown in 10% FBS (*top*) and 0% FBS (*bottom*). Cells were stained in crystal violet solution and solubilized with Sorenson's buffer and quantitated at absorbance of 570 nm. Experiments were done in triplicate. *D*, the ability of EVI1 and MDS1/EVI1 to alter cellular migration was assessed in both serum-free and complete serum conditions in OVCA432 cells (*top*) and T80 cells (*bottom*). The cells that migrated onto the lower surface of the membrane were both photographed and counted. Experiments were done in triplicate.

The effects of MDS1/EVI1 and EVI1 on motility have not been previously reported. Thus, to investigate a potential role in cellular migration, we used both T80 (a normal ovarian immortalized cell line) as well as an ovarian cancer cell line (OVCA432 cells). OVCA432 cells had very low basal migration in the presence of FBS, which facilitates the detection of increases in cellular migration upon transfection with EVI1 and MDS1/EVI1. T80 and OVCA432 ovarian cancer cells were transiently transfected with EVI1 and MDS1/EVI1. Cells were plated into Boyden chambers to assess directional migration using 10% FBS as a chemoattractant. Both EVI1 and MDS1/EVI1 promoted ovarian cell migration, identifying a novel process not previously attributed to EVI1 (Fig. 3*D*, *top* and *bottom*). Thus, transient expression of EVI1 and MDS1/EVI1 exerts similar effects on proliferation and cell motility, increasing both coordinately. We also assessed other ovarian cell lines, including immortalized T29 ovarian epithelial cells, which had slightly increased growth with transfected EVI1; however, motility was not dramatically or significantly increased. T29 as compared with T80 have undergone many of the components of EMT being more fibroblastoid, motile, and invasive in matrigel, potentially contributing to the difference in response.

Because EVI1 inhibits TGFβ-mediated signaling (23), we addressed whether EVI1 and MDS1/EVI1 could modulate TGFβ-mediated plasminogen activator inhibitor-1 (PAI-1) expression,

which reduces cell migration and invasion in breast and gynecologic cancer cells (28), using TGFβ-responsive PAI-1 reporters (PAI-1 and CAGA). In T80 cells and T29 cells, we observed that enforced expression of both EVI1 and MDS1/EVI1 markedly inhibited TGFβ-mediated induction of the PAI-1 promoter (Supplementary Fig. S1) similar to results from others (18). However, enforced expression of MDS1/EVI1 in T29 cells (results not shown) not only did not repress TGFβ-induced CAGA luciferase activity, but increased TGFβ-induced CAGA activity in contrast to EVI1, which repressed the promoter. Because the PAI-1 promoter contains elements that are not present in the CAGA promoter and the CAGA promoter represents a multimerized sequence, the differential effects on the two promoters may be due to the presence of additional regulatory elements in the PAI-1 promoter.

Collectively, these data implicate an important and unexpected role for MDS1/EVI1 and EVI1 in epithelial-mesenchymal transformation in ovarian cancer, specifically the migration of ovarian epithelial cells possibly through induction of PAI-1, thus implicating these gene products in multiple roles in ovarian cancer metastasis.

The PR domain of MDS1/EVI1 is negative for methyltransferase activity. MDS1/EVI1 has been shown to exhibit similar functions or to act as an inhibitor of EVI1 depending on the system investigated (22, 29–31). MDS1/EVI1 (PRDM3) has a novel PR (PRD1-BF1-RIZ homology) domain not present in either MDS1 or EVI1, which has the potential to act as a protein methyltransferase (32). However, using free histones and [^{3}H]-*S*-adenosyl-methionine, we were unable to detect significant differences between the methyltransferase activity associated with MDS1/EVI1 and EVI1 following forced expression in COS7 cells (Fig. 4). In contrast, GST-PRMT1, a type I protein arginine methyltransferase, dramatically increased the methylation of free histone substrates. There was a weak methyltransferase activity associated with both MDS1/EVI1 and EVI1 immunoprecipitates that could be due to coimmunoprecipitation of components of the Swi/Snf complex including BRG1 (SMARCA4; ref. 33) that bind EVI1 and have methyltransferase activity. Together, the data suggest that the PR domain of MDS1/EVI1 does not have methyltransferase activity nor is inactive with the substrates assessed and under conditions where other PR domains are active. The PR domain in MDS1/EVI1 has been reported to inhibit oligomerization and CtBP recruitment (34) and, thus, the ability to inhibit TGFβ signaling in some models, suggesting an alternative mechanism for the differential effects of MDS1/EVI1 and EVI1.

EVI1 and MDS1/EVI1 DNA and RNA correlate with patient prognosis. It has been previously reported that high EVI1 expression in AML patients predicts poor survival in acute myeloid leukemia (AML), whereas MDS1/EVI1 expression correlates with improved outcomes (35). To determine whether overexpression of EVI1 and MDS1/EVI1 correlated with patient outcomes in ovarian cancers, Kaplan-Meier curves using EVI1 DNA and mRNA expression as a categorical variable were generated. We show that overall survival of ovarian cancer patients with elevated DNA copy number of EVI1 was significantly longer ($P < 0.03$) than patients with low levels (Fig. 5*A*). The 0.37 cutoff corresponds to a normalized gain of one copy of the DNA. Overall survival for patients with elevated total EVI1 and MDS1/EVI1 (using exon III probes) or MDS1/EVI1 RNA levels (using MDS1/EVI1-specific probe) was significantly longer ($P < 0.05$) than patients with low EVI1 and MDS1/EVI1 RNA levels (Fig. 5*B*), which is consistent with the CGH data. However, overall survival for patients with elevated EVI1 (using EVI1 exon I probe, which detects EVI1d specifically) was significantly shorter ($P < 0.05$) than patients with low EVI1 RNA levels (Fig. 5*B*), which is similar

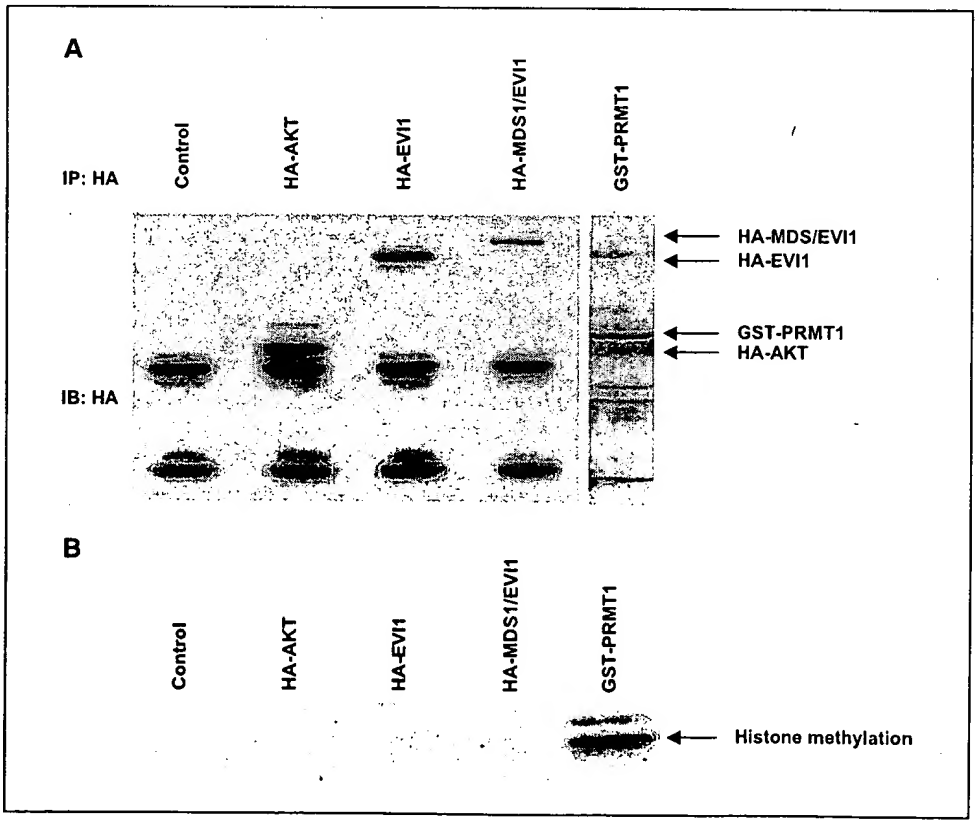

Figure 4. The PR domain of MDS1/EVI1 is negative for methyltransferase activity. *A*, transient transfection with HA-AKT, HA-EVI1, and HA-MDS1/EVI1 fusion constructs was done in COS7 cells. Immunoprecipitation with 12CA5 HA antibody was done 48 h post-transfection and verified by Western analysis using HA antibody. *B*, *in vitro* methyltransferase activity was assessed by incubation of free histones [H3, H4 (F3, F2a1), arginine-rich], purified GST-PRMT1 or HA-tagged proteins/complexes, and [^{3}H]-*S*-adenosyl-L-methyl-methionine. We were unable to detect significant differences between a weak methyltransferase activity associated with MDS1/EVI1-HA immunoprecipitates and EVI1-HA immunoprecipitates. In contrast, GST-PRMT1, a type I protein arginine methyltransferase (46), dramatically increased the methylation of free histone substrates.

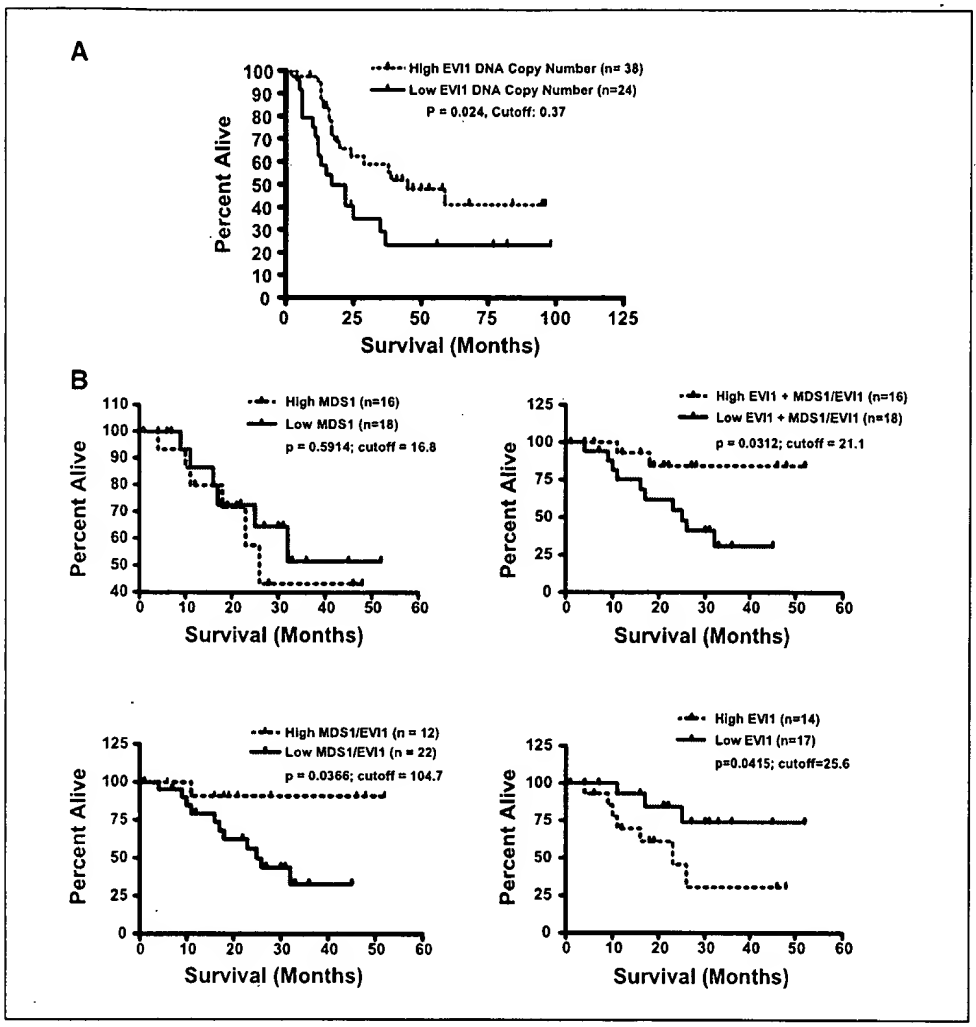

Figure 5. EVI1 and MDS1/EVI1 DNA correlate with good patient prognosis. *A*, increase in EVI1 DNA copy number is an indicator of good prognosis. Overall survival in patients (for patients where survival data were available) with high (>1 copy number increase) EVI1 copy number ($n = 38$) was significantly better ($P < 0.03$) than patients with low EVI1 copy number ($n = 24$). *B*, increase in EVI1 RNA expression is associated with an increased overall survival in ovarian cancer patients. Overall survival in stage III/IV serous epithelial ovarian cancer patients with high total EVI1 and MDS1/EVI1 (exon III primer assessing both EVI1 and MDS1/EVI1) or MDS1/EVI1 RNA levels was significantly better ($P < 0.05$) than patients with low total EVI1 and MDS1/EVI1 or MDS1/EVI1 RNA levels. Overall survival in stage III/IV serous epithelial ovarian cancer patients with high EVI1 (exon I primer assessing only EVI1) was significantly worse ($P < 0.05$) than patients with low EVI1 RNA levels.

to the pattern observed in AML where high EVI1 expression (using EVI1-specific probe against EVI1d) predicts poor patient survival and was associated with the presence of unfavorable cytogenetic abnormalities, whereas MDS1/EVI1 was associated with a favorable karyotype (27). The cutoff value represents the fold-RNA increase at which the *P* value is most significant by iterative analysis of splitting sample sets into high and low. In comparison to ovarian cancers where EVI1 and MDS1/EVI1 transcript levels were dramatically elevated (up to 300-fold), total EVI1 and MDS1/EVI1 transcripts were elevated to a much lesser degree in lung cancer (only up to 20-fold; data not shown). However, despite the modest increase, elevated EVI1 (representing total EVI1 and MDS1/EVI1) levels as assessed by transcriptional profiling (neither MDS1 nor the MDS1/EVI1 intergenic fusion are available in the data set) also indicated good prognosis in lung cancer patients (ref. 36; $n = 86$, $P < 0.05$). Thus, it would seem that MDS1/EVI1 correlates with good prognosis in epithelial cancers not limited to ovary, whereas EVI1 is an indicator of poor patient prognosis in epithelial cancers. However, analysis of additional data sets will be necessary to determine generality across tumor lineages.

Long-term expression of EVI1 and MDS1/EVI1 in immortalized normal ovarian epithelial cells and OVCAR8 cells. To better understand the association of EVI1 and MDS1/EVI1 with patient prognosis, we attempted to generate stable cell lines, including immortalized normal ovarian epithelial cells (T29 and T80) and ovarian cancer cell lines (OVCA420 and OVCAR8). However, using plasmid-based expression systems for both EVI1 and MDS1/EVI1, we were consistently unable to generate stable cell clones. In colony-forming assays with G418 and puromycin selection, the number of stable clones obtained were nonexistent or dramatically reduced compared with vector control. None of the clones expressed the transgenes as analyzed by Western blotting or when expanded survived. Further efforts in generating stable cell lines with EVI1 in OVCAR8 and T29 cells with the retroviral expression vector (pLEGFP-C1) led to the generation of a few EVI1 clones, which were senescent or failed to survive beyond two to three passages. We further attempted to generate stable cell lines using pBABE-puro retroviral expression vectors in OVCAR8 and T29 cells. However, expression of EVI1 in the retroviral pool population was dramatically reduced with passaging even in the presence of antibiotic (puromycin) selection. Thus, it seems that prolonged expression of EVI1 and MDS1/EVI1, in contrast to transient expression, may inhibit cellular proliferation, a process that has been noted with other tumor-promoting genes, such as RAS (37). Thus, these observations suggest that prolonged expression of high levels of EVI1 and MDS1/EVI1 inhibits cellular growth and may contribute to the good prognosis associated with expression of MDS1/EVI1.

Discussion

Regions of chromosomal aberrations frequently harbor novel oncogenes, and thus, the identification of the drivers of these aberrations provides important information for understanding the initiation, progression, and management of cancer. Indeed, our previous studies of genomic amplifications at 3q26 in ovarian cancer identified PIK3CA (11) and PKCι (12, 13) as potential markers of prognosis and therapeutic targets involved in ovarian cancer. The high frequency of activating mutations in PIK3CA in breast and other cancers has confirmed its role as an oncogene (38–41), and parallel studies implicate PKCι as an oncogene in lung cancer (14).

EVI1 has previously been implicated as an oncogene due to the formation of fusion genes with AML1 in AML and MDS (19). However, we have failed to detect evidence for the presence of AML1-MDS1 or AML1-EVI1 fusion genes in ovarian cancer. We now show by high-resolution CGH analysis that EVI1 is located at the center of the minimally aberrant region at 3q26.2, one of the earliest and most frequent genomic amplifications in ovarian cancer. Furthermore, we show that this DNA copy number increase is associated with a marked accumulation of both EVI1 and MDS1/EVI1 (PRDM3) intergenic read-through transcripts in ovarian cancers. The marked increase in RNA levels compared with the modest increase in copy number suggests that mechanisms in addition to genomic amplification contribute to the deregulation of these genes. Acquisition of structural aberrations within the promoters of EVI1 or MDS1 during the rearrangement that accompanies amplification or epigenetic events such as hypomethylation, which has been reported for PRDM16 (MEL1S) in leukemia (42), may contribute to this deregulation. Nevertheless, both RNA and protein levels of MDS1/EVI1 and EVI1 are markedly aberrant in the majority of ovarian cancers.

EVI1 gene copy number and MDS1/EVI1 transcript levels are associated with increased survival duration, whereas EVI1d-specific transcript levels are associated with reduced survival duration in ovarian cancer patients. We have identified a number of splice variants of EVI1,[7] which may account for the poor prognosis associated with the amplification of EVI1 in ovarian cancers. It is currently unclear why the MDS1/EVI1 transcript in ovarian cancers is associated with favorable patient prognosis; however, the difficulty in developing stable MDS1/EVI1-expressing cell lines suggests that long-term expression may limit tumor expansion. EVI1 and MDS1/EVI1 proteins have been reported to exhibit both partially antagonistic and similar biological properties. In our assays, although both EVI1 and MDS1/EVI1 behaved similarly in migration and proliferation studies, and furthermore, that the MDS1/EVI1 PR domain was negative for methyltransferase activity, we did observe that MDS1/EVI1 activated the CAGA promoter in contrast to the repressive effect of EVI1. The altered effects of the constructs may contribute to the differential effects on outcomes. Because TGFβ initially limits tumor formation by inhibiting proliferation and inducing apoptosis but increases the metastatic capacity of advanced tumors (43), blockade of TGFβ signaling by MDS1/EVI1 could increase the likelihood of tumor development but result in a less aggressive tumor, which would be sufficient to explain the increased tumor frequency as well as the improved outcome associated with 3q26 amplification. Furthermore, as indicated by both RNA and protein assays, MDS1/EVI1 seems to be increased in ovarian cancer to a much greater degree than EVI1. Indeed, in a recent study designed to identify genes that may play a role in the resistance of ovarian cancer cells to TGFβ, EVI1 was identified as amplified and overexpressed and to inhibit TGFβ signaling in immortalized ovarian epithelium (18). Importantly, however, these studies did not distinguish between whether EVI1 or MDS1/EVI1 was involved. It remains possible that MDS1/EVI1 or EVI1 is amplified as a prerequisite for the induction of a nearby gene such as SnoN/SkiL as it has been recently reported that SnoN is transcriptionally induced by EVI1 (44). In addition, whereas EVI1 is clearly involved in the prognosis of leukemia, EVI1 transgenic mice failed to develop leukemia, suggesting that cooperating events may be necessary for the full manifestation of the actions of EVI1 or MDS1/EVI1 (45). Indeed, the 3q26.2 amplicon is complex, and cooperating events between genes within this region or with other regions of genomic aberrations may be necessary for the full expression of ovarian tumorigenesis. Taken together, these findings provide a potential explanation for the observation that genomic amplification of MDS1/EVI1 and EVI1 is associated with an improved outcome.

Interfering with EVI1 or MDS1/EVI1 expression or function could have therapeutic utility as >95% of ovarian cancers express elevated mRNA levels. However, the association of the MDS1/EVI1 with an improved outcome suggests that this approach needs to be explored with care. Selective inhibition of EVI1, as it is associated with a worsened outcome, may be beneficial. In addition, the MDS1/EVI1 fusion protein may represent a novel target for immunotherapy or for early diagnosis. The outcomes of the studies described herein may potentially apply broadly to epithelial tumors where the 3q26.2 aberration is present (ovary, breast, head and neck, cervix, and lung) as well as in leukemias.

[7] M. Nanjundan and G.B. Mills, unpublished observations.

Acknowledgments

Received 6/28/2006; revised 11/30/2006; accepted 1/29/2007.

Grant support: National Cancer Institute P50 CA083639 and P30 CA16672 (G.B. Mills), P01 CA64602 (G.B. Mills and J.W. Gray), and in part by the U.S. Department of Energy, Office of Science, Office of Biological and Environmental Research (Contract DE-AC03-76SF00098, J.W. Gray).

The costs of publication of this article were defrayed in part by the payment of page charges. This article must therefore be hereby marked *advertisement* in accordance with 18 U.S.C. Section 1734 solely to indicate this fact.

References

1. Sugita M, Tanaka N, Davidson S, et al. Molecular definition of a small amplification domain within 3q26 in tumors of cervix, ovary, and lung. Cancer Genet Cytogenet 2000;117:9–18.
2. Imoto I, Yuki Y, Sonoda I, et al. Identification of ZASC1 encoding a Kruppel-like zinc finger protein as a novel target for 3q26 amplification in esophageal squamous cell carcinomas. Cancer Res 2003;63:5691–6.
3. Imoto I, Pimkhaokham A, Fukuda Y, et al. SNO is a probable target for gene amplification at 3q26 in squamous-cell carcinomas of the esophagus. Biochem Biophys Res Commun 2001;286:559–65.
4. Riazimand SH, Welkoborsky HJ, Bernauer HS, Jacob R, Mann WJ. Investigations for fine mapping of amplifications in chromosome 3q26.3–28 frequently occurring in squamous cell carcinomas of the head and neck. Oncology 2002;63:385–92.
5. Sattler HP, Rohde V, Bonkhoff H, Zwergel T, Wullich B. Comparative genomic hybridization reveals DNA copy number gains to frequently occur in human prostate cancer. Prostate 1999;39:79–86.
6. Sattler HP, Lensch R, Rohde V, et al. Novel amplification unit at chromosome 3q25–27 in human prostate cancer. Prostate 2000;45:207–15.
7. Weber-Mangal S, Sinn HP, Popp S, et al. Breast cancer in young women (< or = 35 years): genomic aberrations detected by comparative genomic hybridization. Int J Cancer 2003;107:583–92.

8. Wessels LF, van Welsem T, Hart AA, van't Veer LJ, Reinders MJ, Nederlof PM. Molecular classification of breast carcinomas by comparative genomic hybridization: a specific somatic genetic profile for BRCA1 tumors. Cancer Res 2002;62:7110–7.
9. Or YY, Hui AB, Tam KY, Huang DP, Lo KW. Characterization of chromosome 3q and 12q amplicons in nasopharyngeal carcinoma cell lines. Int J Oncol 2005; 26:49–56.
10. Casas S, Aventin A, Fuentes F, et al. Genetic diagnosis by comparative genomic hybridization in adult *de novo* acute myelocytic leukemia. Cancer Genet Cytogenet 2004;153:16–25.
11. Shayesteh L, Lu Y, Kuo WL, et al. PIK3CA is implicated as an oncogene in ovarian cancer. Nat Genet 1999;21:99–102.
12. Eder AM, Sui X, Rosen DG, et al. Atypical PKCι contributes to poor prognosis through loss of apical-basal polarity and cyclin E overexpression in ovarian cancer. Proc Natl Acad Sci U S A 2005;102:12519–24.
13. Zhang L, Huang J, Yang N, et al. Integrative genomic analysis of protein kinase C (PKC) family identifies PKCι as a biomarker and potential oncogene in ovarian carcinoma. Cancer Res 2006;66:4627–35.
14. Regala RP, Weems C, Jamieson L, et al. Atypical protein kinase Cι is an oncogene in human non-small cell lung cancer. Cancer Res 2005;65:8905–11.
15. Guan XY, Fung JM, Ma NF, et al. Oncogenic role of eIF-5A2 in the development of ovarian cancer. Cancer Res 2004;64:4197–200.
16. Estilo CL, O-Charoenrat P, Ngai I, et al. The role of novel oncogenes squamous cell carcinoma-related oncogene and phosphatidylinositol 3-kinase p110α in squamous cell carcinoma of the oral tongue. Clin Cancer Res 2003;9:2300–6.
17. Yokoi S, Yasui K, Iizasa T, Imoto I, Fujisawa T, Inazawa J. TERC identified as a probable target within the 3q26 amplicon that is detected frequently in non-small cell lung cancers. Clin Cancer Res 2003;9:4705–13.
18. Sunde JS, Donninger H, Wu K, et al. Expression profiling identifies altered expression of genes that contribute to the inhibition of transforming growth factor-β signaling in ovarian cancer. Cancer Res 2006;66: 8404–12.
19. Nucifora G, Laricchia-Robbio L, Senyuk V. EVI1 and hematopoietic disorders: history and perspectives. Gene 2006;368:1–11.
20. Liu Y, Chen L, Ko TC, Fields AP, Thompson EA. Evi1 is a survival factor which conveys resistance to both TGFβ- and taxol-mediated cell death via PI3K/AKT. Oncogene 2006;25:3565–75.
21. Snijders AM, Nowak N, Segraves R, et al. Assembly of microarrays for genome-wide measurement of DNA copy number. Nat Genet 2001;29:263–4.
22. Vinatzer U, Taplick J, Seiser C, Fonatsch C, Wieser R. The leukaemia-associated transcription factors EVI-1 and MDS1/EVI1 repress transcription and interact with histone deacetylase. Br J Haematol 2001;114:566–73.
23. Kurokawa M, Mitani K, Irie K, et al. The oncoprotein Evi-1 represses TGF-β signalling by inhibiting Smad3. Nature 1998;394:92–6.
24. Tanaka T, Nishida J, Mitani K, Ogawa S, Yazaki Y, Hirai H. Evi-1 raises AP-1 activity and stimulates c-fos promoter transactivation with dependence on the second zinc finger domain. J Biol Chem 1994;269: 24020–6.
25. Morishita K, Parganas E, Douglass EC, Ihle JN. Unique expression of the human Evi-1 gene in an endometrial carcinoma cell line: sequence of cDNAs and structure of alternatively spliced transcripts. Oncogene 1990;5:963–71.
26. Brooks DJ, Woodward S, Thompson FH, et al. Expression of the zinc finger gene EVI-1 in ovarian and other cancers. Br J Cancer 1996;74:1518–25.
27. Barjesteh van Waalwijk van Doorn-Khosrovani S, Erpelinck C, van Putten WL, et al. High EVI1 expression predicts poor survival in acute myeloid leukemia: a study of 319 *de novo* AML patients. Blood 2003;101:837–45.
28. Whitley BR, Palmieri D, Twerdi CD, Church FC. Expression of active plasminogen activator inhibitor-1 reduces cell migration and invasion in breast and gynecological cancer cells. Exp Cell Res 2004;296:151–62.
29. Sood R, Talwar-Trikha A, Chakrabarti SR, Nucifora G. MDS1/EVI1 enhances TGF-β1 signaling and strengthens its growth-inhibitory effect but the leukemia-associated fusion protein AML1/MDS1/EVI1, product of the t(3;21), abrogates growth-inhibition in response to TGF-β1. Leukemia 1999;13:348–57.
30. Soderholm J, Kobayashi H, Mathieu C, Rowley JD, Nucifora G. The leukemia-associated gene MDS1/EVI1 is a new type of GATA-binding transactivator. Leukemia 1997;11:352–8.
31. Vinatzer U, Mannhalter C, Mitterbauer M, et al. Quantitative comparison of the expression of EVI1 and its presumptive antagonist, MDS1/EVI1, in patients with myeloid leukemia. Genes Chromosomes Cancer 2003;36: 80–9.
32. Steele-Perkins G, Fang W, Yang XH, et al. Tumor formation and inactivation of RIZ1, an Rb-binding member of a nuclear protein-methyltransferase superfamily. Genes Dev 2001;15:2250–62.
33. Chi Y, Senyuk V, Chakraborty S, Nucifora G. EVI1 promotes cell proliferation by interacting with BRG1 and blocking the repression of BRG1 on E2F1 activity. J Biol Chem 2003;278:49806–11.
34. Nitta E, Izutsu K, Yamaguchi Y, et al. Oligomerization of Evi-1 regulated by the PR domain contributes to recruitment of corepressor CtBP. Oncogene 2005;24: 6165–73.
35. Barjesteh van Waalwijk van Doorn-Khosrovani S, Erpelinck C, Lowenberg B, Delwel R. Low expression of MDS1-1-like-1 (MEL1) and EVI1-like-1 (EL1) genes in favorable-risk acute myeloid leukemia. Exp Hematol 2003;31:1066–72.
36. Beer DG, Kardia SL, Huang CC, et al. Gene-expression profiles predict survival of patients with lung adenocarcinoma. Nat Med 2002;8:816–24.
37. Maldonado JL, Timmerman L, Fridlyand J, Bastian BC. Mechanisms of cell-cycle arrest in Spitz nevi with constitutive activation of the MAP-kinase pathway. Am J Pathol 2004;164:1783–7.
38. Campbell IG, Russell SE, Phillips WA. PIK3CA mutations in ovarian cancer. Clin Cancer Res 2005;11: 7042; author reply 42–3.
39. Wang Y, Helland A, Holm R, Kristensen GB, Borresen-Dale AL. PIK3CA mutations in advanced ovarian carcinomas. Hum Mutat 2005;25:322.
40. Campbell IG, Russell SE, Choong DY, et al. Mutation of the PIK3CA gene in ovarian and breast cancer. Cancer Res 2004;64:7678–81.
41. Levine DA, Bogomolniy F, Yee CJ, et al. Frequent mutation of the PIK3CA gene in ovarian and breast cancers. Clin Cancer Res 2005;11:2875–8.
42. Yoshida M, Nosaka K, Yasunaga J, Nishikata I, Morishita K, Matsuoka M. Aberrant expression of the MEL1S gene identified in association with hypomethylation in adult T-cell leukemia cells. Blood 2004;103: 2753–60.
43. Elliott RL, Blobe GC. Role of transforming growth factor β in human cancer. J Clin Oncol 2005;23:2078–93.
44. Yatsula B, Lin S, Read AJ, et al. Identification of binding sites of EVI1 in mammalian cells. J Biol Chem 2005;280:30712–22.
45. Louz D, van den Broek M, Verbakel S, et al. Erythroid defects and increased retrovirally-induced tumor formation in Evi1 transgenic mice. Leukemia 2000;14: 1876–84.
46. Frankel A, Yadav N, Lee J, Branscombe TL, Clarke S, Bedford MT. The novel human protein arginine *N*-methyltransferase PRMT6 is a nuclear enzyme displaying unique substrate specificity. J Biol Chem 2002;277: 3537–43.